

Supporting Material for

A silicon nanocrystals/polymer nanocomposite as down-conversion layer in organic and hybrid solar cells

V. Svrcek¹, T. Yamanari¹, D. Mariotti², S. Mitra², T. Velusamy², K. Matsubara¹

¹Research Center for Photovoltaics, National Institute of Advanced Industrial Science and Technology (AIST), Central 2, Umezono 1-1-1, Tsukuba, 305-8568, Japan

²Nanotechnology & Integrated Bio-Engineering Centre (NIBEC), University of Ulster, UK

S1. Photoluminescence and quantum yield of surface-engineered silicon nanocrystals

The microplasma treatment of silicon nanocrystals (Si-ncs) directly in ethanol has been extensively studied and reported in our previous publications [1-5]. Here we include unpublished results that confirm photoluminescence (PL) results and report on the quantum yield (QY) of the Si-ncs before and after the microplasma treatment. Both PL and QY measurements support the conclusions on surface modification discussed by Mariotti *et al.* [4]. The measured PL intensity has been enhanced by 8 to 10 times after 30 min plasma processing and the PL wavelength was red-shifted by ~70 nm (figure S1), similarly to our previous work [4, 5].

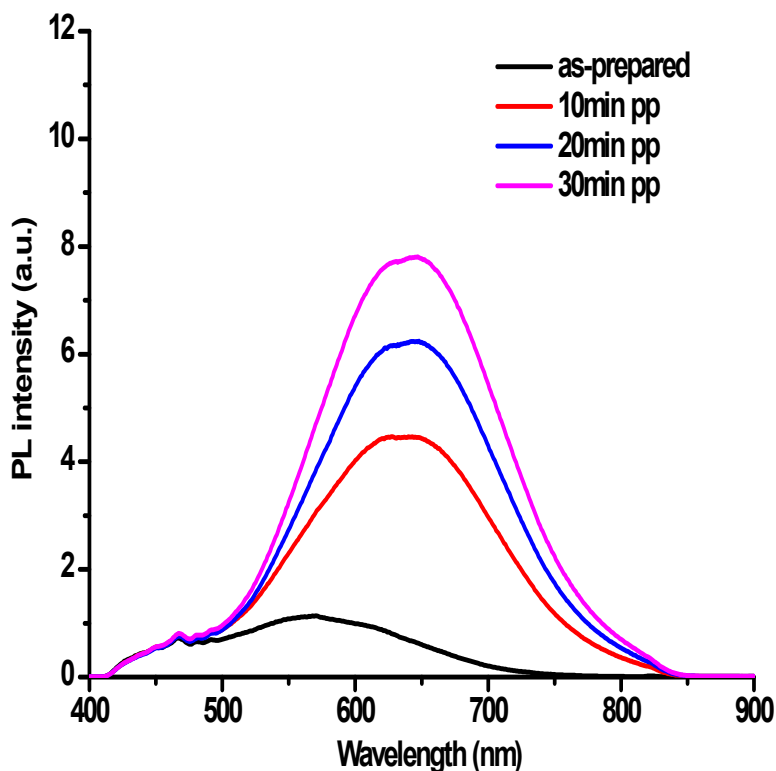


Figure S1. Photoluminescence (PL) of silicon nanocrystals (Si-ncs) in ethanol after radio frequency (RF) microplasma processing. Here, “pp” signifies “plasma processing”.

QY was measured by taking the ratio of the number of emitted photons with the number of absorbed photons. The method is reported for instance by Mangolini *et al.* and de Mello *et al.* [6, 7]. In the present study, a customized PL QY system has been used and includes an integrating sphere (Horiba Scientific). The integrating sphere is connected to an ultraviolet (UV) laser diode and a *Fluoromax-4 Horiba Jobin-Yvon* spectrofluorometer through an optic fiber.

Following the procedure reported in the main manuscript, processed and unprocessed samples of Si-ncs in ethanol were drop-casted and dried on a Si wafer for 1 h at room temperature. Initially a baseline measurement is taken by introducing only a Si wafer. After the baseline measurement, the samples with the processed and unprocessed Si-ncs were introduced in the integrating sphere. The QY can then be easily calculated [6, 7].

	Unprocessed Si-ncs	Processed Si-ncs
Quantum Yield	10.1%	29.3%

Table S1. Quantum yield of Si nanocrystals (Si-ncs) in ethanol.

In Table S1, it can be noticed that after processing, the QY of Si-ncs has been enhanced by about three times. This confirms that microplasma-induced surface engineering has the capability of introducing improved optical properties. As mentioned in the main manuscript, the initial 10% QY is relatively modest and QYs above 80% could be achieved using optimized Si-ncs produced for instance by plasmas [8, 9].

S2. Materials characterization of silicon nanocrystals

The Si-ncs produced by electrochemical etching and used for this work have undergone extensive characterization in the past years and we have been consistent in using the same process for a number of years which has produced results in good agreement with the existing literature on porous silicon (e.g. see Supporting Information in [4]). Detailed characterization of our Si-ncs before processing can be found in our published work and corresponding supporting information; these contain Fourier transform infrared spectroscopy [1, 4, 5, 10-13], X-ray photoelectron spectroscopy [3, 10], transmission electron microscopy (TEM) [2, 4]. Detailed characterization of our Si-ncs after microplasma processing in ethanol can be found in our published work and corresponding supporting information; these contain Fourier transform infrared spectroscopy [4, 5], X-ray photoelectron spectroscopy [3], transmission electron microscopy [2, 4]. The comparison between a direct-current microplasma process and a radio-frequency microplasma process has been also studied for Si-ncs in water [1]. Here we include additional TEM images (figure S2) and X-ray diffraction analysis (XRD; figure S3), the latter used to estimate the average crystal size.

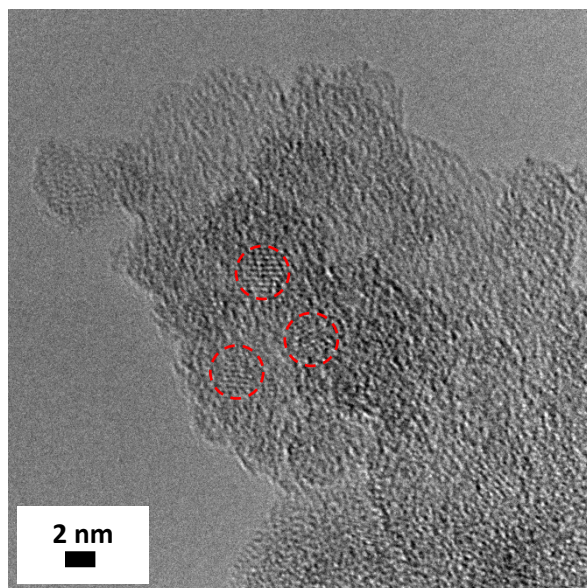


Figure S2. Transmission electron microscopy images of electrochemically etched silicon nanocrystals; dashed red circles identify nanocrystals exhibiting typical crystalline fringes.

Figure S2 shows a typical TEM image of the electrochemically etched Si-ncs (see references [2, 4] for more images). The simultaneous identification of several nanocrystals is complicated by the aggregated state of the powder which prevents the microscope to focus on several Si-ncs at the same time. In this case, at least three Si-ncs can be observed (dashed red circles) which show crystalline fringes and a diameter between 2 nm and 3 nm. Because each TEM image can only show very few nanocrystals at the same time, size distribution by TEM is a difficult task; the assessment of the size is therefore better performed with XRD where the TEM images can support the analysis.

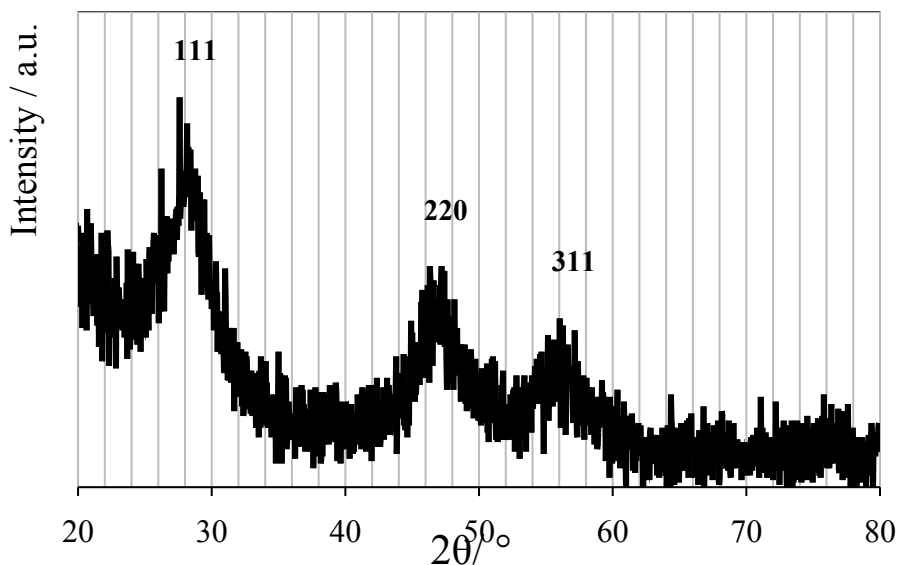


Figure S3. X-ray diffraction of as-prepared silicon nanocrystals.

The XRD analysis confirm that Si-ncs are crystalline with face-centred cubic structures (PDF: 261481; FCC, Cubic; $a = 5.43 \text{ \AA}$). The particle size can be estimated from XRD data using the Debye-Scherrer method [14] and for our samples the calculations produced a value of about 2 nm, which confirm our previous findings. We have verified that the microplasma process only affects the surface and therefore crystal structure and size distribution are expected to remain the same after the treatment [2, 4].

S3. Characterization of the polymer and nanocomposite films

The Si-ncs/PEDOT:PSS nanocomposite has been recently investigated by our groups and results published elsewhere [10]. Structural analysis of the Si-ncs/PEDOT:PSS composites showed microplasma surface engineered Si-ncs to be well dispersed within PEDOT:PSS. On the other hand the optical properties of PTB7:PCBM and PTB7 were separately investigated as well. Figure S4 presents absorption spectra of the PTB7:PCBM and PTB7. Absorption spectrum of the glass substrate is also shown for comparison.

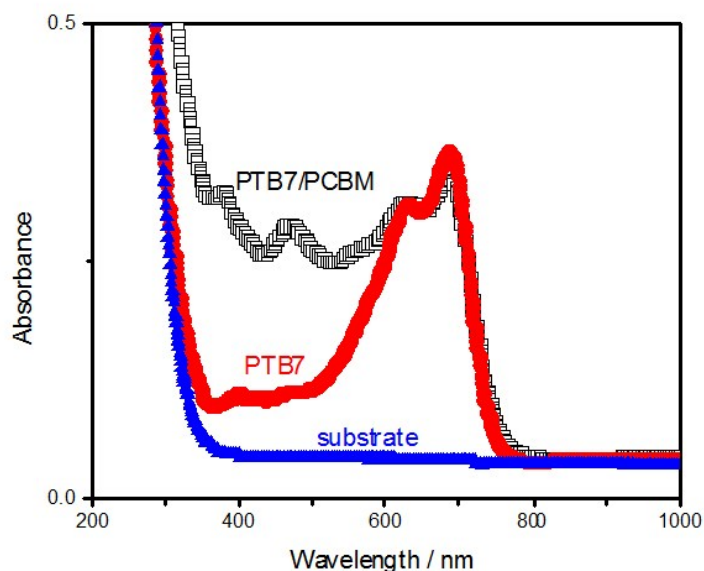


Figure S4. Absorption spectra of the PTB7:PCBM and PTB7. Absorption spectrum of the glass substrate is also shown for comparison.

References

- [1] Mitra S, Švrček V, Mariotti D, Velusamy T., Matsubara K, Kondo M *Plas. Proc. and Polym.* **11** (2014) 158
- [2] Švrček V, Dohnalova K, Mariotti D, Trinh M T, Limpens R, Mitra S, Gregorkiewicz T, Matsubara K, Kondo M *Adv. Fun. Mat.* **23** (2013) 6051
- [3] Švrček V, Mariotti D, Mitra S, Kaneko T, Li L, Cvelbar U, Matsubara K, Kondo M *Journal of Physical Chemistry C* **117** (2013) 10939
- [4] Mariotti D, Švrček V, Hamilton J W J, Schmidt M, Kondo M *Adv. Funct. Mat.* **22** (2012) 954
- [5] Švrček V, Mariotti D, Kondo M *Appl. Phys. Lett.* **97** (2010) 161502
- [6] Mangolini L, Jurbergs D, Rogojina E, Kortshagen U *J. Lumin.* **121** (2006) 327
- [7] de Mello JC, Wittmann HF, Friend RH *Adv. Mater.* **9** (1997) 230
- [8] Miller JB, van Sickle AR, Anthony RJ, Kroll DM, Kortshagen UR, Hobbie EK *ACS Nano* **6** (2012) 7389
- [9] Askari S, Levchenko I, Ostrikov K, Maguire P, Mariotti D *Appl. Phys. Lett.* **104** (2014) 163103.

- [10] Mitra S, Cook S, Švrček V, Blackley R A, Wuzong Z, Kovač J, Cvelbar U, Mariotti D *J. of Phys. Chem. C* **117** (2013) 23198
- [11] Švrček V, Mariotti D, Kalia K, Dickinson C, Kondo M *J. of Phys. Chem. C* **115** (2011) 6235
- [12] Švrček V, Mariotti D, Nagai T, Shibata Y, Turkevych Y, Kondo M *J. of Phys. Chem. C* **115** (2011) 5084
- [13] McKenna J, Patel J, Mitra S, Soin N, Švrček V, Mariotti D *The Eur. Phys. J-Appl. Phys.* **56** (2011) 24020
- [14] Debye P, von Röntgenstrahlen *Z Ann. Phys.* **351** (1915) 809
- [15] Švrček V, Yamanari T, Mariotti D, Matsubara K, Kondo M. *Appl. Phys. Lett.* **100**, (2012) 223904.